INSTITUT NATIONAL DE RECHERCHE EN INFORMATIQUE ET EN AUTOMATIQUE

Bifurcations and periodic motion induced by the Painlevé paradox

Remco Leine — Bernard Brogliato

N° 4322

Décembre 2001

THÈME 4

Rapport de recherche

ISSN 0249-6399 ISRN INRIA/RR--4322--FR+ENG

Bifurcations and periodic motion induced by the Painlevé paradox

Remco Leine[*] , Bernard Brogliato

Thème 4 — Simulation et optimisation
de systèmes complexes
Projet Bip

Rapport de recherche n° 4322 — Décembre 2001 — 48 pages

Abstract: In this report we study the periodic motion and bifurcations of the Frictional Bounce Model, which consists of an object with normal and tangential degrees of freedom that comes in contact with a rigid surface. The Frictional Bounce Model contains the basic mechanism for a hopping phenomenon observed in many practical applications. We will show that the hopping or bouncing motion in this type of systems is closely related to the Painlevé paradox. A dynamical system exhibiting the Painlevé paradox has nonuniqueness and nonexistence of solutions in certain sliding modes. Furthermore, we will show that this type of systems can exhibit the Painlevé paradox for physically realistic values of the friction coefficient.

Key-words: nonuniqueness, multibody dynamics, linear complementarity problem, contact

[*] Department of Mechanical Engineering, Eindhoven University of Technology, P.O. Box 513, 5600 MB Eindhoven, The Netherlands, Email: r.i.leine@tue.nl

Unité de recherche INRIA Rhône-Alpes
655, avenue de l'Europe, 38330 Montbonnot-St-Martin (France)
Téléphone : +33 4 76 61 52 00 — Télécopie +33 4 76 61 52 52

Bifurcations et mouvement peŕiodique introduit par le paradoxe de Painlevé

Résumé : Dans ce rapport, nous étudions le mouvement périodique et les bifurcations du 'Frictional Bounce Model'. Ce modèle est constitué d'un corps rigide avec des degrés de liberté dans les directions normale et tangentielle, en contact avec une surface rigide. Le 'Frictional Bounce Model' contient le mécanisme essentiel pour le phenomène de broutage, qui conduit à faire rebondir le solide contre la paroi. Nous demontrons que le phenomène de broutage dans ce type de systèmes est relié au paradoxe de Painlevé. Le paradoxe de Painlevé, dans de tels systèmes dynamiques, conduit à la non-unicité et la non-existence des solutions dans certains modes de glissement. En outre, nous demontrons que ce type de systémes peut exhiber le paradoxe de Painlevé pour des paramètres physiques réalistes du coefficient de frottement.

Mots-clés : non-unicité, dynamique des multi-corps, problème linéaire de complémentarité, contact

1 Introduction

If a finger is pushed over a table, then a hopping motion of the finger can be observed when the finger and table are sufficiently rough. The same phenomenon occurs when a piece of chalk is push over the blackboard, often resulting in a dotted line which indicates periodic detachment. Brake systems, consisting of a pin-on-disk mechanism, can exhibit an intermittent motion, where the pin periodically looses contact with the disk, accompanied by a squealing noise [14]. Robotic manipulators, which touch a surface of an obstacle, may also show a kind of bouncing motion, normally regarded as undesirable [2]. In this paper we will study the Frictional Bounce Model, which consists of an object with normal and tangential degrees of freedom that comes in contact with a rigid surface. The Frictional Bounce Model contains the basic mechanism for the hopping phenomenon observed in many practical applications. We will show that the hopping or bouncing motion in this type of systems is closely related to the Painlevé paradox (which we explain the the sequel). Furthermore, we will show that this type of systems can exhibit the Painlevé paradox for arbitrary (positive) values of the friction coefficient.

The rigid multibody theory [2,9,11,27,32], which assumes instantaneous impact between rigid bodies and Amontons-Coulomb friction model in tangential direction, provides a good approach to study the dynamics when one is interested in the global motion of the system. Mechanical systems with friction and impact, modelled with a rigid multibody approach, belong therefore to the class of hybrid systems (i.e. systems with a mixed continuous and discrete nature in time). The transitions in time from one hybrid mode to another (e.g. from contact to detachment or stick to slip) demand the choice of the next hybrid mode. A rigorous way to perform this search is to formulate the problem as a Linear Complementarity problem (LCP). The solution of the LCP can be nonunique, giving an undeterminate next hybrid mode, and the solution of the LCP may even not exist, which leads to inconsistency in the model. The occurrence of inconsistency in a mechanical rigid multibody system due to friction is known as the *Painlevé paradox.*

It has been known since the end of the 19th century that the combination of Amontons-Coulomb friction together with the assumption of rigidity can cause inconsistencies for high values of the friction coefficient [15, 29, 30]. Painlevé [29, 30] considered the sliding motion of rigid objects [1] in contact with the ground, which have inconsistencies in the sliding mode. The problem of a sliding rod studied by Painlevé became the classical example of a hybrid system with inconsistencies. Lecornu [17] proposed velocity jumps to escape from inconsistent modes, often now addressed as impacts without collisions. A number of studies show that inconsistencies occur in the classical Painlevé example when the friction coefficient μ is larger than $\frac{4}{3}$ [9, 23, 24]. The classical Painlevé example was recently studied in more detail in [8]. New results on how the solution passes singular points in the sliding mode were presented in [8].

[1] The original example studied by Painlevé in [30] (1895) is that of a box on an inclined plane. A brief description of the original example of Painlevé is given in Appendix A. The classical example of Painlevé, being a sliding rod, was studied in [30] (1905).

The critical value of $\frac{4}{3}$ is very large and not likely to occur in physical situations. In [7] an adapted version of the classical Painlevé example was proposed, where the rod has a rounded tip, which lowers the critical friction coefficient to 0.63 (the example with a rounded tip was inspired by Moreau [26]). The original example studied by Painlevé [30], being the contact of a box with the ground, can have a much lower critical friction coefficient for a small radius of gyration (see Appendix A). The occurrence of the Painlevé paradox of a rigid body with a friction rotor was studied in [37, 38] and a critical friction coefficient was found which can take arbitrary (positive) values depending on other parameters. A similar conclusion is drawn in the present paper.

A model of a hopping finger was studied by Moreau [26]. Stick-slip motion with and without flight phase were reported, as well period-doubled motion, but the occurrence of the Painlevé paradox was not studied. The Frictional Bounce Model, presented in the present paper, is slightly different and lends itself better for an analytical investigation of the Painlevé paradox.

Control of the sliding motion of an end-effector of a robot on the surface of an obstacle can be hampered by the same instability phenomena which govern the Frictional Bounce Model. The results on the Frictional Bounce Model, which will be studied in the sequel, can help to design better control schemes for constrained robotic motion.

Unilateral contact laws, as are used in the rigid multibody approach, lead to nonsmooth mathematical models due to their set-valued nature. Bifurcations in smooth systems are well understood [12] but little is known about bifurcations in nonsmooth systems [21]. Literature on bifurcations in nonsmooth mechanical systems seems to be divided in two groups:

1. Bifurcations in systems with *friction*, which belong to the class of Filippov-systems. Literature on this topic is vast (for instance [3,6,18,19,33,35,36,39]). A general theory for bifurcations in Filippov-systems is not available but attempts to explore in that direction are made [4, 20, 21].

2. Bifurcations in systems with *impact* [5, 13, 25, 28, 31]. The impacts are almost always considered to be frictionless and the systems very often contain only a single contact.

Literature on bifurcations in systems with multiple contacts with combined friction and impact is hardly available. An impact oscillator with friction is studied in [1] but the impact and friction are in different contact points for this system and the contact problem is therefore decoupled. Mechanical systems with combined impact and friction are studied in [22] and bifurcation diagrams are constructed with the aid of a one-dimensional Poincaré map. The topic of bifurcations which are created by the Painlevé paradox has up to now not been addressed in literature and will be studied in the present paper.

The main results on the classical Painlevé example will be briefly discussed in Section 3. The Frictional Bounce Model will be studied in Section 4. This model can be simplified which leads to the Simplified Frictional Bounce Model (Section 5). Critical friction coefficients of the Painlevé paradox will be derived for both models and numerical results for the periodic solutions will be given. Bifurcations diagrams of the models are presented in Section 6.

The notation as well as the methods of [9, 32] are used for the dynamics of rigid multibody systems with impact and friction and are reviewed in in Section 2.

2 Mathematical Modeling of Impact with Friction

In this section we will briefly review some aspects of a mathematical theory for the dynamics of rigid bodies with completely inelastic frictional impact as has been formulated in [9,11,32]. A shorter version of this formulation can be found in [22].

For the description on the dynamics of multibody systems it is convenient to introduce four contact sets, which describe the kinematic state of the constraints of the system:

$$\begin{array}{ll} I_G = \{1, 2, \ldots, n_G\} & \\ I_S = \{i \in I_G \mid g_{Ni} = 0\} & \text{with } n_S \text{ elements} \\ I_N = \{i \in I_S \mid \dot{g}_{Ni} = 0\} & \text{with } n_N \text{ elements} \\ I_H = \{i \in I_N \mid \dot{g}_{Ti} = 0\} & \text{with } n_H \text{ elements,} \end{array} \tag{2.1}$$

where g_{Ni} and $\dot{g}_{Ti}$ denote the normal contact distance and tangential relative velocity of constraint i. The set I_G consists of n_G indices of all constraints, which we want to take into account. I_S contains the n_S indices of the constraints with vanishing normal distance but arbitrary relative velocity. In the set I_N are the n_N indices of the potentially active normal constraints, which fulfill the necessary conditions for continuous contact (vanishing normal distance and no relative velocity in normal direction). The set I_N contains therefore all indices of slipping or sticking contacts. The n_H elements of the set I_H correspond to the potentially active constraints in tangential direction (sticking). The sets I_S, I_N, I_H are not constant, because the contact configuration of the dynamical system changes with time due to stick-slip transitions, impact and contact loss.

The dynamics of a multibody system can be expressed for almost all t by the equation of motion

$$\boldsymbol{M}(t,\boldsymbol{q})\ddot{\boldsymbol{q}} - \boldsymbol{h}(t,\boldsymbol{q},\dot{\boldsymbol{q}}) - \sum_{i \in I_S} (\boldsymbol{w}_N(t,\boldsymbol{q})\lambda_N + \boldsymbol{w}_T(t,\boldsymbol{q})\lambda_T)_i = \boldsymbol{0}, \tag{2.2}$$

where $\boldsymbol{M}$ is the symmetric mass matrix, $\boldsymbol{q}$ the vector of generalized coordinates, $\boldsymbol{h}$ the vector with all smooth elastic, gyroscopic and dissipating generalized forces and $\boldsymbol{\lambda}_N$ and $\boldsymbol{\lambda}_T$ the vectors with normal and tangential contact forces. The vectors $\boldsymbol{w}_N$ and $\boldsymbol{w}_T$ are the normal and tangential force directions.

We assume the generalized coordinates $\boldsymbol{q}(t)$ to be absolute continuous functions in time and the generalized velocities $\dot{\boldsymbol{q}}(t)$ to be functions of locally bounded variations, when a solution exists of course. We therefore can define the left and right limits $\dot{\boldsymbol{q}}(t^-)$ and $\dot{\boldsymbol{q}}(t^+)$ at each time instant $t > t_0$. Furthermore, we assume the generalized velocities to be right-continuous, i.e. $\dot{\boldsymbol{q}}(t) = \dot{\boldsymbol{q}}(t^+)$. We specify the initial condition at $t = t_0$ by $(\boldsymbol{q}_0, \dot{\boldsymbol{q}}_0) = (\boldsymbol{q}(t_0), \dot{\boldsymbol{q}}(t_0))$. If we allow a first velocity jump to occur at t_0 then we set $\dot{\boldsymbol{q}}_0 = \dot{\boldsymbol{q}}(t_0^-)$. Typically, the contact forces λ_N and λ_T become impulsive when an impact occurs and we have $\dot{\boldsymbol{q}}(t^-) \neq \dot{\boldsymbol{q}}(t^+)$.

More conveniently we put (2.2) in the form

$$\boldsymbol{M}\ddot{\boldsymbol{q}} - \boldsymbol{h} - \boldsymbol{W}_N\boldsymbol{\lambda}_N - \boldsymbol{W}_T\boldsymbol{\lambda}_T = \boldsymbol{0} \tag{2.3}$$

where the dependencies on $t, \boldsymbol{q}, \dot{\boldsymbol{q}}$ have been omitted for brevity and where $\boldsymbol{W}_N$ and $\boldsymbol{W}_T$ are matrices containing the generalized force directions in normal and tangential direction. The contact distances g_{Ni} and g_{Ti} are gathered in the vectors $\boldsymbol{g}_N$ and $\boldsymbol{g}_T$. We can express the contact velocities and accelerations in the generalized accelerations by

$$\begin{bmatrix} \dot{\boldsymbol{g}}_N \\ \dot{\boldsymbol{g}}_T \end{bmatrix} = \begin{bmatrix} \boldsymbol{W}_N^{\mathrm{T}} \\ \boldsymbol{W}_T^{\mathrm{T}} \end{bmatrix} \dot{\boldsymbol{q}} + \begin{bmatrix} \tilde{\boldsymbol{w}}_N \\ \tilde{\boldsymbol{w}}_T \end{bmatrix}, \qquad \begin{bmatrix} \ddot{\boldsymbol{g}}_N \\ \ddot{\boldsymbol{g}}_T \end{bmatrix} = \begin{bmatrix} \boldsymbol{W}_N^{\mathrm{T}} \\ \boldsymbol{W}_T^{\mathrm{T}} \end{bmatrix} \ddot{\boldsymbol{q}} + \begin{bmatrix} \bar{\boldsymbol{w}}_N \\ \bar{\boldsymbol{w}}_T \end{bmatrix}. \tag{2.4}$$

Each closed contact $i \in I_N$ is characterized by a vanishing contact distance g_{Ni} and normal relative velocity $\dot{g}_{Ni}$. Under the assumption of impenetrability $g_{Ni} \geq 0$, only two situations may occur:

$$\begin{array}{ll} \ddot{g}_{Ni} = 0 \wedge \lambda_{Ni} \geq 0 & \text{contact is maintained} \\ \ddot{g}_{Ni} > 0 \wedge \lambda_{Ni} = 0 & \text{detachment} \end{array} \tag{2.5}$$

From (2.5) we see that the normal contact law shows a complementary behaviour: the product of the contact force and acceleration is always zero:

$$\ddot{g}_{Ni}\lambda_{Ni} = 0, \qquad i \in I_N. \tag{2.6}$$

The complementary behaviour of the normal contact law is depicted in Figure 2.1a and shows a corner of admissible combinations of $\ddot{g}_{Ni}$ and λ_{Ni}.

We assume Amontons-Coulomb law to hold in the tangential direction. For a closed contact $i \in I_N$, with friction coefficient μ_i, the following three cases are possible:

$$\begin{array}{lcll} \dot{g}_{Ti} = 0 & \Rightarrow & |\lambda_{Ti}| \leq \mu_i\lambda_{Ni} & \text{sticking} \\ \dot{g}_{Ti} < 0 & \Rightarrow & \lambda_{Ti} = +\mu_i\lambda_{Ni} & \text{negative sliding} \\ \dot{g}_{Ti} > 0 & \Rightarrow & \lambda_{Ti} = -\mu_i\lambda_{Ni} & \text{positive sliding} \end{array} \qquad i \in I_N. \tag{2.7}$$

To determine the tangential contact force during sticking, one can formulate unilateral laws for sticking contacts. For a closed sticking contact $i \in I_H$ the following three cases are possible

$$\begin{array}{lcll} \ddot{g}_{Ti} = 0 & \Rightarrow & |\lambda_{Ti}| \leq \mu_i\lambda_{Ni} & \text{remains sticking} \\ \ddot{g}_{Ti} < 0 & \Rightarrow & \lambda_{Ti} = +\mu_i\lambda_{Ni} & \text{commences negative sliding} \\ \ddot{g}_{Ti} > 0 & \Rightarrow & \lambda_{Ti} = -\mu_i\lambda_{Ni} & \text{commences positive sliding} \end{array} \qquad i \in I_H. \tag{2.8}$$

The normal and tangential contact law lead, together with the equations of motion, to the coupled normal–tangential contact problem for the stick-slip and detachment transitions of the multibody system

$$\begin{bmatrix} \ddot{\boldsymbol{g}}_N \\ \ddot{\boldsymbol{g}}_H \end{bmatrix} = \begin{bmatrix} \boldsymbol{W}_N^{\mathrm{T}}\boldsymbol{M}^{-1}(\boldsymbol{W}_N + \boldsymbol{W}_G\boldsymbol{\mu}_G) & \boldsymbol{W}_N^{\mathrm{T}}\boldsymbol{M}^{-1}\boldsymbol{W}_H \\ \boldsymbol{W}_H^{\mathrm{T}}\boldsymbol{M}^{-1}(\boldsymbol{W}_N + \boldsymbol{W}_G\boldsymbol{\mu}_G) & \boldsymbol{W}_H^{\mathrm{T}}\boldsymbol{M}^{-1}\boldsymbol{W}_H \end{bmatrix} \begin{bmatrix} \boldsymbol{\lambda}_N \\ \boldsymbol{\lambda}_H \end{bmatrix} + \begin{bmatrix} \boldsymbol{W}_N^{\mathrm{T}}\boldsymbol{M}^{-1}\boldsymbol{h} + \bar{\boldsymbol{w}}_N \\ \boldsymbol{W}_H^{\mathrm{T}}\boldsymbol{M}^{-1}\boldsymbol{h} + \bar{\boldsymbol{w}}_H \end{bmatrix} \tag{2.9}$$

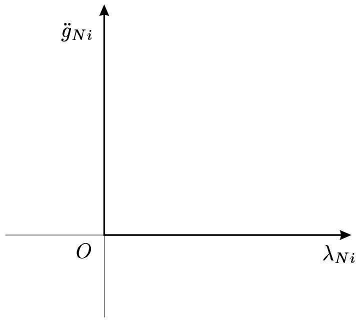

(a) normal direction

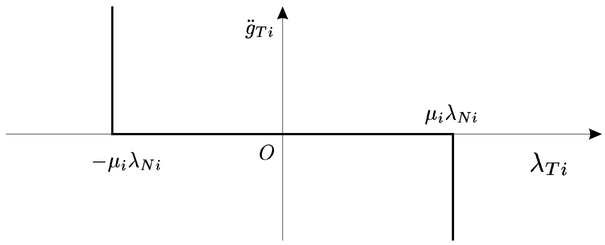

(b) tangential direction

Figure 2.1: Complementarity of contacts.

with[2]

$$\begin{array}{ll} 0 \leq \ddot{\boldsymbol{g}}_N \perp \boldsymbol{\lambda}_N \geq 0 & \in I_N \\ \boldsymbol{\lambda}_H \in -\boldsymbol{\mu}_H \boldsymbol{\lambda}_N \mathrm{diag}(\partial |\ddot{\boldsymbol{g}}_H|) & \in I_H \end{array} \tag{2.10}$$

where

$$\begin{array}{c} \boldsymbol{W}_G = \boldsymbol{w}_{Ti}, \qquad i \in I_N \backslash I_H, \\ \boldsymbol{g}_H = g_{Ti}, \quad \boldsymbol{\lambda}_H = \lambda_{Ti}, \quad \boldsymbol{W}_H = \boldsymbol{w}_{Ti}, \quad \bar{\boldsymbol{w}}_H = \bar{w}_{Ti}, \qquad i \in I_H \\ \boldsymbol{\mu}_H \in \mathbb{R}^{n_H \times n_N}, \quad \boldsymbol{\mu}_G \in \mathbb{R}^{n_N - n_H \times n_N} \end{array} \tag{2.11}$$

and where the subdifferential of convex analysis $\partial|x| = \mathrm{Sign}(x)$ has been used. Equations (2.9) can be transformed into an LCP as has been formulated in [9, 32].

If an impact occurs, then we generally have a discontinuity of in the generalized velocities $\dot{\boldsymbol{q}}$. The impact is assumed to begin at a time t^- and to end at a time t^+. The time difference $t^+ - t^-$ is assumed to be "infinitely small"[3] in the rigid multibody approach. The equation of motion is integrated over the impact time

$$\boldsymbol{M}\big(\dot{\boldsymbol{q}}(t^+) - \dot{\boldsymbol{q}}(t^-)\big) = \begin{bmatrix} \boldsymbol{W}_N & \boldsymbol{W}_T \end{bmatrix} \begin{bmatrix} \boldsymbol{\Lambda}_N \\ \boldsymbol{\Lambda}_T \end{bmatrix}, \tag{2.12}$$

which yields the velocity jump $\dot{\boldsymbol{q}}(t^+) - \dot{\boldsymbol{q}}(t^-)$ as a function of the impulses $\boldsymbol{\Lambda}_N$ and $\boldsymbol{\Lambda}_T$ in normal and tangential direction defined by

$$\Lambda_{Ni} = \lim_{t^+ \to t^-} \int_{t^-}^{t^+} \lambda_{Ni} dt, \qquad \Lambda_{Ti} = \lim_{t^+ \to t^-} \int_{t^-}^{t^+} \lambda_{Ti} dt, \qquad i \in I_S. \tag{2.13}$$

[2]The notation $\boldsymbol{a} \perp \boldsymbol{b}$ means that $\boldsymbol{a}$ stands perpendicular to $\boldsymbol{b}$, i.e. $\boldsymbol{a}^{\mathrm{T}}\boldsymbol{b} = 0$. It follows therefore from the complementarity conditions $\boldsymbol{0} \leq \boldsymbol{a} \perp \boldsymbol{b} \geq \boldsymbol{0}$, that if $a_i > 0$ then $b_i = 0$ and vice versa.

[3]Mathematically more correct is to consider the impact as a singleton, i.e. a point in time, and the equation of motion as a measure differential equation, which is beyond the scope of this paper (see [10, 27]).

Due to the unilateral character of the contact constraint only nonnegative normal contact forces are possible, $\lambda_{Ni} \geq 0$, which results in nonnegative values of the normal impulses $\Lambda_{Ni} \geq 0$. At the end of the completely inelastic impact the approaching process of the bodies has to be completed. Thus negative values of the contact velocities are forbidden, $\dot{g}_{Ni}(t^+) \geq 0$. If an impulse is transferred ($\Lambda_{Ni} > 0$), then the corresponding contact participates in the impact and $\dot{g}_{Ni}(t^+) = 0$. If no impulse is transferred ($\Lambda_{NCi} = 0$), then the corresponding constraint is superfluous and we allow velocities $\dot{g}_{Ni}(t^+) \geq 0$. The impact law in normal direction is therefore expressed by the complementarity condition

$$\Lambda_{Ni} \geq 0, \quad \dot{g}_{Ni}(t^+) \geq 0, \quad \Lambda_{Ni}\dot{g}_{Ni}(t^+) = 0; \quad i \in I_S. \tag{2.14}$$

Possible stick-slip transitions during the collision with reversed sliding prevent an analytical integration of Coulomb's friction law (2.8) over the impact time interval. However, we state the tangential impact law as

$$\begin{array}{llll} \dot{g}_{Ti}(t^+) = 0 & \Rightarrow & |\Lambda_{Ti}| \leq \mu_i \Lambda_{Ni} & \text{sticking} \\ \dot{g}_{Ti}(t^+) < 0 & \Rightarrow & \Lambda_{Ti} = +\mu_i \Lambda_{Ni} & \text{negative sliding} \\ \dot{g}_{Ti}(t^+) > 0 & \Rightarrow & \Lambda_{Ti} = -\mu_i \Lambda_{Ni} & \text{positive sliding} \end{array} \qquad i \in I_S. \tag{2.15}$$

with the remark that (2.15) coincides with Coulomb's friction law (2.8) in the cases of continuous sliding during the impact and of arbitrary transitions to sticking at the end of the impact. Only events of reversed sliding or transitions from sticking to sliding with a sliding phase at the end of the impact are different from Coulomb's law [9, 27, 32].

Evaluating the contact velocities (2.4) at t^+ and t^- gives

$$\begin{bmatrix} \dot{\boldsymbol{g}}_N(t^+) \\ \dot{\boldsymbol{g}}_T(t^+) \end{bmatrix} = \begin{bmatrix} \boldsymbol{W}_N^{\mathrm{T}} \\ \boldsymbol{W}_T^{\mathrm{T}} \end{bmatrix} \left(\dot{\boldsymbol{q}}(t^+) - \dot{\boldsymbol{q}}(t^-)\right) + \begin{bmatrix} \dot{\boldsymbol{g}}_N(t^-) \\ \dot{\boldsymbol{g}}_T(t^-) \end{bmatrix} \qquad \in \mathbb{R}^{2n_S}. \tag{2.16}$$

Substitution of (2.12) in (2.16) together with the contact laws (2.14) and (2.15) gives the set of equations

$$\begin{bmatrix} \dot{\boldsymbol{g}}_N(t^+) \\ \dot{\boldsymbol{g}}_T(t^+) \end{bmatrix} = \begin{bmatrix} \boldsymbol{W}_N^{\mathrm{T}}\boldsymbol{M}^{-1}\boldsymbol{W}_N & \boldsymbol{W}_N^{\mathrm{T}}\boldsymbol{M}^{-1}\boldsymbol{W}_T \\ \boldsymbol{W}_T^{\mathrm{T}}\boldsymbol{M}^{-1}\boldsymbol{W}_N & \boldsymbol{W}_T^{\mathrm{T}}\boldsymbol{M}^{-1}\boldsymbol{W}_T \end{bmatrix} \begin{bmatrix} \boldsymbol{\Lambda}_N \\ \boldsymbol{\Lambda}_T \end{bmatrix} + \begin{bmatrix} \dot{\boldsymbol{g}}_N(t^-) \\ \dot{\boldsymbol{g}}_T(t^-) \end{bmatrix} \tag{2.17}$$

with

$$\begin{array}{rl} 0 \leq \dot{\boldsymbol{g}}_N(t^+) \perp \boldsymbol{\Lambda}_N \geq 0 & \in I_S \\ \boldsymbol{\Lambda}_T \in -\boldsymbol{\mu}_S \boldsymbol{\Lambda}_N \mathrm{diag}(\partial|\dot{\boldsymbol{g}}_T(t^+)|) & \in I_S, \end{array} \tag{2.18}$$

where $\boldsymbol{\mu}_S = \mathrm{diag}(\mu_i), i \in I_S$. The formulation of the coupled normal-tangential contact problem for completely inelastic impact is given by (2.17) and is usually solved by reformulating it as an LCP.

In the sequel we will use an event-driven integration scheme to obtain solutions $\boldsymbol{q}(t)$ of unilaterally constrained mechanical systems. The equation of motion (2.3) for given index sets is numerically integrated until an impact, stick-slip or detachment event occurs. If the event is an impact event, then the impact equations (2.17) have to be solved, after which the